Available online at www.sciencedirect.com
SCIENCE DIRECT®
Journal of Power Sources 141 (2005) 216–226
JOURNAL OF POWER SOURCES
www.elsevier.com/locate/jpowsour

Optimisation of processing and microstructural parameters of LSM cathodes to improve the electrochemical performance of anode-supported SOFCs

V.A.C. Haanappel*, J. Mertens, D. Rutenbeck, C. Tropartz, W. Herzhof, D. Sebold, F. Tietz

Institute for Materials and Processes in Energy Systems, Forschungszentrum Jülich, 52425 Jülich, Germany

Received 13 April 2004; received in revised form 7 September 2004; accepted 27 September 2004
Available online 21 November 2004

Abstract

To improve the electrochemical performance of LSM-based anode-supported single cells, a systematic approach was taken for optimising processing and materials parameters. Four parameters were investigated in more detail: (1) the LSM/YSZ mass ratio of the cathode functional layer, (2) the grain size of LSM powder for the cathode current collector layer, (3) the thickness of the cathode functional layer and the cathode current collector layer, and (4) the influence of calcination of YSZ powder used for the cathode functional layer.

Results from electrochemical measurements performed between 700 and 900 °C with H_2 (3 vol.% H_2O) as fuel gas and air as the oxidant showed that the performance was the highest using an LSM/YSZ mass ratio of 50/50. A further increase of the electrochemical performance was obtained by increasing the grain size of the outer cathode current collector layer: the highest performance was achieved with non-ground LSM powder. In addition, it was found that the thickness of the cathode functional layer and cathode current collector layer also affects the electrochemical performance, whereas no obvious detrimental effects occurred with the different qualities of YSZ powder for the cathode functional layer. The highest performance, i.e. $1.50 \pm 0.05\,A\,cm^{-2}$ at 800 °C and 700 mV, was obtained with a cathode functional layer, characterised by an LSM/YSZ mass ratio of 50/50, a d_{90} of the LSM powder of 1.0 μm, non-calcined YSZ powder, and a thickness of about 30 μm, and a cathode current collector layer, characterised by d_{90} of the LSM powder of 26.0 μm (non-ground), and a thickness of 50–60 μm. Also interesting to note is that the use of non-ground LSM for the cathode current collector layer and non-calcined YSZ powder for the cathode functional layer obviously simplifies the production route of this type of fuel cell.

Keywords: Solid oxide fuel cells (SOFC); Cathode; LSM; Microstructure; Anode-supported.

1. Introduction

One of the main targets in the development of anode-supported or planar solid oxide fuel cells (SOFCs) is to lower the operation temperature. A lower operation temperature involves several advantages, such as the use of cheaper materials for interconnects and manifolds, reduced sealing and corrosion problems, and increased lifetime and reliability. This will finally result in reaching a basis for commercial viability.

However, in order to maintain the power output without affecting the output voltage of SOFC systems at lower operation temperatures, an increase of the electrochemical performance is needed. This can be achieved by optimising processing and microstructural parameters of existing SOFCs or by using other materials for the electrolyte and cathode.

Significant progress in this direction was already made several years ago by the introduction of anode-supported instead of electrolyte-supported SOFCs [1]. The "state-of-the-art" anode-supported single cells manufactured at Forschungszentrum Jülich are characterised by a double-layered $La_{0.65}Sr_{0.3}MnO_3$ (LSM)/LSM–Y_2O_3-stabilised ZrO_2 (YSZ) cathode applied on a thin YSZ electrolyte [1]. These LSM-

* Corresponding author. Tel.: +49 2461 614656; fax: +49 2461 616770.
E-mail address: v.haanappel@fz-juelich.de (V.A.C. Haanappel).

0378-7753/$ – see front matter © 2004 Elsevier B.V. All rights reserved.
doi:10.1016/j.jpowsour.2004.09.016

based cathodes are generally used for SOFCs operating at relatively high temperatures, i.e. between 800 and 1000 °C. Lowering the temperature significantly reduces the current density since the cathode reactions become the limiting factor for the power output of the SOFC. Studies have already been initiated in order to improve the oxygen transfer processes, and thus to enhance the current density [2–10]. In those studies, the following processing and microstructural parameters were varied:

- the LSM/YSZ ratio of the cathode functional layer (CFL);
- the average grain size and grain size distribution of the CFL and cathode current collector layer (CCCL);
- the thickness of the CFL and CCCL;
- the porosity of the CFL and CCCL;
- the extent of a graded interface of the CFL;
- production techniques to apply the CFL and CCCL.

A first attempt to modify the LSM-based cathode was made by Kenjo and Nishiya [2]. From that study it was concluded that mixing the LSM cathode with YSZ significantly improves the electrochemical performance due to an increase of the effective reaction surface area. Subsequent studies dealt with different cathode microstructures and fabrication methods, see for example Refs. [3–10].

Other studies focused on improving the oxide ion conductivity of the electrolyte by developing and/or by optimising different types of materials, such as lanthanum gallate-based oxides partly replaced by strontium and magnesium [11–16], YSZ [17–20], and ceria partly replaced by samarium, gadolinium, calcium, and yttrium [15,21–28].

Apart from this, the addition of small amounts of noble metals, e.g. Pd, Ag, or Pt, to the cathode can improve the oxygen exchange reaction [17,26,29–39] as well. Others started to use different cathode materials to achieve a higher performance; e.g. $BaCoO_3$ [40], (La, Sr)(Fe, Co)$O_{3-\delta}$ [21,22,24,29,31,37,41–44], (La, Sr)(Co, Cu)$O_{3-\delta}$ [36,45], and (Sm, Sr)CoO_3 [46]. More information about the use of several cathode and electrolyte materials can also be found in reviews, such as Refs. [47,48].

In most of the studies concerning a modification of the LSM-based cathode half-cells were employed for investigation and characterisation by measuring the polarisation resistance using electrochemical impedance spectroscopy [2,5–10]. Nevertheless, the data obtained give a well-argued input to modify complete SOFCs in a systematic way, finally resulting in a better performance.

To provide the highest possible electrochemical performance of anode-supported single cells with an LSM-based cathode, next to the main requirements for the cathode [6], such as, high electronic conductivity, high electro-catalytic activity, chemical compatibility, matching expansion coefficient and good adherence to the electrolyte, the following additional requirements have to be considered:

- Because the electrochemical performance strongly depends on the effective length of the triple phase boundary (TPB) LSM–YSZ–oxygen, the total length of this TPB in the CFL has to be as large as possible. This can be achieved by optimising the LSM/YSZ ratio (according to the percolation theory), the use of small grains of the LSM and YSZ powder, and by increasing the thickness of the CFL.
- The porosity of the CFL and the CCCL should be as large as possible, this in order to maximise gas diffusion.
- A minimum thickness of the CCCL is necessary in order to fully utilize the total surface area of the interface. In the case the thickness of the current collector is too small in relation to the distance between the contact points of the Pt-mesh, it cannot be ensured that the current is collected from the whole LSM/LSM–YSZ interface area.
- The thickness of the CFL and CCCL should be kept as small as possible. The polarization resistance can be detrimentally affected by applying a CFL and/or CCCL with a too large thickness.

Based on these requirements, a systematic approach was set up in order to investigate the influence of (a) the LSM/YSZ mass ratio of the CFL, (b) the grain size of the CCCL, (c) the thickness of the CFL and CCCL, and (d) YSZ powder calcination (for the CFL) on the electrochemical performance of LSM-based anode-supported single cells.

2. Experimental

2.1. Preparation of cells

Anode-supported single cells with a dimension of 50 mm × 50 mm consisted of an anode substrate (thickness: ~1500 μm), an anode functional layer (thickness: 5–10 μm) and an electrolyte (thickness: 5–10 μm). The anode substrate, a porous composite consisting of NiO (Baker, USA) and zirconia stabilised with 8 mol% yttria (8YSZ) (Unitec, UK), was produced by warm pressing using a so-called Coat-Mix® material and pre-sintered at 1200 °C [1,15,16]. Afterwards, the anode functional layer (NiO/8YSZ) and the electrolyte (8YSZ (Tosoh, Japan)) were both deposited by vacuum slip casting and co-fired at 1400 °C [17]. The CFL with LSM and 8YSZ (Tosoh, Japan) as base materials and the CCCL (LSM) were applied by screen-printing on the top of the electrolyte. The area of both layers, also indicated as the active surface area, was 40 mm × 40 mm.

Pastes for the screen-printing process to apply the cathode layers were prepared by mixing the corresponding powders with a binder consisting of ethyl cellulose in terpineol. More details concerning the different powders/pastes used for the screen-printed CFL and CCCL are listed in Table 1.

The LSM powder used for both cathode layers was synthesised by a spray-drying process [1,18] using nitrate salts, i.e. $La(NO_3)_3{\cdot}6H_2O$, $Sr(NO_3)_2$, and $Mn(NO_3)_2{\cdot}4H_2O$, followed by a calcination step at 900 °C for 3 h to obtain the perovskite structure.

Table 1
Overview of pastes used for screen-printed CFL and CCCL

Type	Substrate	Grain size (μm)			Mass ratio
		d_{10}	d_{50}	d_{90}	LSM/YSZ
CFL					
CFL-A1	LSM	0.23	0.52	0.91	30/70
	8YSZ (calcined)	0.16	0.40	1.04	
CFL-A2	LSM	0.23	0.52	0.91	40/60
	8YSZ (calcined)	0.16	0.40	1.04	
CFL-A3	LSM	0.23	0.52	0.91	45/55
	8YSZ (calcined)	0.16	0.40	1.04	
CFL-A4	LSM	0.23	0.52	0.91	50/50
	8YSZ (calcined)	0.16	0.40	1.04	
CFL-A5	LSM	0.23	0.52	0.91	55/45
	8YSZ (calcined)	0.16	0.40	1.04	
CFL-A6	LSM	0.23	0.52	0.91	60/40
	8YSZ (calcined)	0.16	0.40	1.04	
CFL-A7	LSM	0.23	0.52	0.91	70/30
	8YSZ (calcined)	0.16	0.40	1.04	
CFL-B1	LSM	0.23	0.52	0.91	50/50
	8YSZ (not calcined)	0.15	0.34	0.92	
CFL-B2	LSM	0.23	0.52	0.91	60/40
	8YSZ (not calcined)	0.15	0.34	0.92	
CCCL					
CCCL-A	LSM	0.34	0.96	2.15	
CCCL-B	LSM	1.00	2.28	4.69	
CCCL-C	LSM	0.39	1.14	2.47	
CCCL-D	LSM	0.73	1.56	3.09	
CCCL-E	LSM	1.16	4.51	10.2	
CCCL-F	LSM	2.18	11.6	26.0	

Performance evaluation of the single cells as a function of various microstructural parameters was done in a systematic way by studying the following series of single cells, i.e.:

- single cells with different LSM/YSZ ratios;
- single cells with different grain size of the CCCL;
- single cells with different thicknesses of the CFL and CCCL;
- single cells with calcined and non-calcined YSZ.

The above listed series are based on using various combinations of pastes for the CFL and CCCL (Table 1).

2.2. Electrochemical measurements

Electrochemical measurements of the single cells were performed in an alumina test housing placed inside the furnace. In order to obtain sufficient electronic contact between the cell and the electronic devices, at the anode side a Ni mesh and at the cathode side a Pt mesh was used. Sealing of the gas compartment was realized by a gold seal. At the beginning of the tests an argon flow was introduced at the anode side and an air flow at the cathode side. The temperature was then slowly increased to the temperature for anode reduction. After reaching this temperature, the anode of the single cells was reduced by a stepwise replacement of argon by hydrogen. Water vapour (3 vol.%) was added by saturating the hydrogen gas through a water bubbler and condenser (super saturation and condensation) at the desired dew point (24 °C). The total gas flows of hydrogen and air were both set at 1000 ml min^{-1} (standard temperature and pressure: STP) using mass flow controllers. The electrochemical performance was measured between 700 and 900 °C. All electrochemical data were obtained by dc methods using a current-control power supply type Gossen 62N–SSP500–40 (Gossen-Metrawatt GmbH, Germany) and a computer-controlled data acquisition system including a datalogger type NetDAQ 2640A (Fluke, The Netherlands). The current–voltage characteristics were measured with increasing current load by a sequential step change of 0.0625 A cm^{-2} starting from zero until the voltage dropped below 0.7 V or until the maximum current load of 1.25 A cm^{-2} was reached. A comparison of the electrochemical performance of the different type of single cells was made by comparing the current densities at 0.7 V. The calculations of the current density at 700 mV (for $I > 1.25$ A cm^{-2}) at exact temperatures, i.e. 700, 750, 800, 850 and 900 °C, are based on inter- or extrapolation using a second or third order polynomial function. Calculations of the area-specific resistance are based on linear regression of the current–voltage curves at 0.7 V.

2.3. Characterisation

The stoichiometry of the LSM powders was controlled by ICP-OES and the phase purity by X-ray diffraction (Siemens

D 500). Grain size distribution measurements of powders were carried out by a Fritsch Analysette 22 with software version 1.8.0. SEM analysis was performed using a LEO 1530 electron microscope.

3. Results

3.1. On the influence of LSM/YSZ ratio

3.1.1. Microstructural parameters

One series of anode-supported cells was produced with a CFL characterised by different mass ratios of LSM/YSZ, i.e. 30/70, 40/60, 50/50, 60/40, and 70/30 (pastes: CFL-A1,2,4,6,7 and CCCL-A). In order to determine the sensitivity of small deviations from the optimum LSM/YSZ ratio, another series was produced with three different mass ratios, i.e. 45/55, 50/50, and 55/45 (pastes: CFL-A3,4,5 and CCCL-B). For both series, the thickness of the CFL and CCCL was kept constant at 10 and 30–35 μm, respectively.

3.1.2. Microstructure

Fig. 1a shows a micrograph of the fracture surface of a single cell with a porous LSM CCCL on the top (paste CCCL-A) with a thickness of about 30–35 μm. Beneath the CCCL, a CFL with a thickness of about 10 μm can be observed, which is based on a mixture of LSM and YSZ having an LSM/YSZ mass ratio of 60/40 (paste CFL-A6). This layer is subsequently followed by a dense YSZ electrolyte with a thickness of 10 μm, an anode functional layer, based on a Ni/YSZ cermet, and the anode substrate (Ni/YSZ). The microstructure of the cells with other LSM/YSZ ratios in the CFL was the same. Therefore, it can be concluded that differences in the electrochemical performance are only due to variations in the LSM/YSZ mass ratio. In Fig. 1b the fracture surface of a single cell is depicted with a CCCL applied with paste CCCL-B. The LSM/YSZ mass ratio of the cathode functional layer was 50/50 (paste CFL-A4). No differences between the microstructures resulted by varying the LSM/YSZ mass ratio between 45/55 and 55/45.

3.1.3. Current–voltage measurements

The average current densities at 700 mV and the area-specific resistance between 700 and 900 °C of single cells prepared with CFL-A1,2,4,6,7 and CCCL-A are given in Table 2. The highest electrochemical performance was obtained with single cells with an LSM/YSZ mass ratio of the CFL of 50/50. Fig. 2 shows the current–voltage curves including power output at 800 °C for the different LSM/YSZ mass ratios.

For single cells with mass ratios of 45/55, 50/50, and 55/45, the average current densities and area-specific resistance are given in Table 3. In this case, the electrochemical performance of the cells with an LSM/YSZ ratio of 55/45 was lower than that found for those with a ratio of 45/55 and

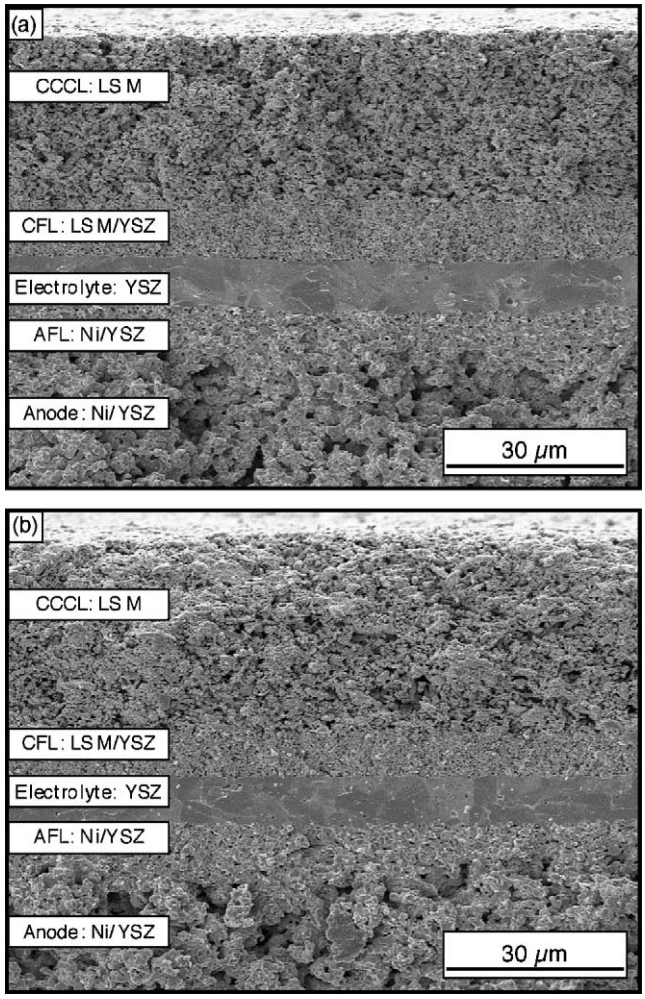

Fig. 1. SEM micrographs of the fracture surface of single cells with a porous LSM CCCL ((a) CCCL-A; (b) CCCL-B) at the top, followed by an LSM/YSZ CFL ((a) CFL-A6; (b) CFL-A4), the electrolyte (YSZ), and the anode substrate including an anode functional layer (Ni/YSZ cermet).

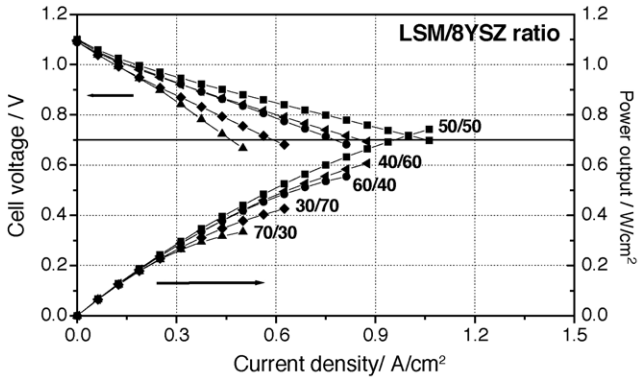

Fig. 2. Current–voltage curves for 16 cm^2 single cells at 800 °C with different LSM/YSZ-ratios (fuel gas: H_2 (3% H_2O) = 1000 ml min^{-1}, oxidant: air = 1000 ml min^{-1}). Cells with different CFLs (CFL-A1,2,4,6,7) and one type of a CCCL (CCCL-A).

Table 2
Average calculated current densities and area-specific resistance of anode-supported single cells with a CFL (thickness: 10 μm) and CCCL (CCCL-A, thickness: 30–35 μm) as a function of the LSM/YSZ mass ratio

Temperature (°C)	30/70 CFL-A1	40/60 CFL-A2	50/50 CFL-A4	60/40 CFL-A6	70/30 CFL-A7
Current density (A cm^{-2} at 700 mV) as a function of LSM/YSZ mass ratio					
900	0.95 ± 0.19	1.21 ± 0.07	1.55 ± 0.32	1.40 ± 0.16	1.12 ± 0.05
850	0.80 ± 0.12	1.11 ± 0.04	1.35 ± 0.23	1.12 ± 0.06	0.77 ± 0.04
800	0.57 ± 0.06	0.86 ± 0.02	1.02 ± 0.15	0.77 ± 0.03	0.47 ± 0.04
750	0.36 ± 0.04	0.56 ± 0.00	0.66 ± 0.08	0.46 ± 0.03	0.28 ± 0.01
700	0.29 ± 0.08	0.35 ± 0.02	0.36 ± 0.03	0.28 ± 0.01	0.17 ± 0.00
Area-specific resistance (mΩ cm^2) as a function of LSM/YSZ mass ratio					
900	331 ± 73	248 ± 14	211 ± 49	241 ± 32	335 ± 8
850	406 ± 73	279 ± 6	239 ± 49	294 ± 20	500 ± 39
800	600 ± 66	378 ± 16	333 ± 56	479 ± 50	864 ± 64
750	1026 ± 99	667 ± 14	558 ± 69	831 ± 50	1443 ± 78
700	1818 ± 30	1179 ± 41	926 ± 81	1328 ± 26	2264 ± 42

50/50, whereas no significant differences occurred between the latter two.

Furthermore, from Tables 2 and 3 it can be concluded that the current density of cells prepared with pastes CFL-A4 and CCCL-A is lower than that of those with CFL-A4 and CCCL-B.

3.2. On the influence of grain size of the CCCL

3.2.1. Microstructural parameters

In order to investigate the effect of different grain sizes of the CCCL on the electrochemical performance, LSM powders with $d_{90,LSM}$ = 2.47, 3.09, 4.69, 10.2, and 26.0 μm, were used (CCCL-C, CCCL-D, CCCL-B, CCCL-E, and CCCL-F, respectively). The LSM/YSZ mass ratio of the CFL based on paste CFL-A6 was 60/40. The thickness of the two cathode layers was 10 and 30–35 μm, as in the former series of cells.

3.2.2. Microstructure

Fig. 3 shows micrographs of the fracture surface of four different types of cells with an LSM/YSZ CFL at the bottom and an LSM CCCL at the top: CCCL-C (a), CCCL-B (b), CCCL-E (c), and CCCL-F (d). From these micrographs it can be observed that with increasing grain size of the LSM powder the pore size increases.

Table 3
Average calculated current densities and area-specific resistance of anode-supported single cells with a CFL (thickness: 10 μm) and CCCL (CCCL-B, thickness: 30–35 μm) as a function of the LSM/YSZ mass ratio

Temperature (°C)	45/55 CFL-A3	50/50 CFL-A4	55/45 CFL-A5
Current density (A cm^{-2} at 700 mV) as a function of LSM/YSZ mass ratio			
900	1.77 ± 0.03	1.81 ± 0.04	1.61 ± 0.03
850	1.58 ± 0.02	1.59 ± 0.03	1.43 ± 0.03
800	1.25 ± 0.01	1.22 ± 0.04	1.11 ± 0.02
750	0.87 ± 0.01	0.79 ± 0.04	0.74 ± 0.02
700	0.55 ± 0.01	0.48 ± 0.02	0.46 ± 0.02
Area-specific resistance (mΩ cm^2) as a function of LSM/YSZ mass ratio			
900	170 ± 1	166 ± 5	186 ± 2
850	196 ± 4	192 ± 3	219 ± 2
800	243 ± 3	240 ± 3	262 ± 3
750	351 ± 6	398 ± 20	406 ± 7
700	560 ± 11	585 ± 29	685 ± 17

3.2.3. Current–voltage measurements

Current densities at 700 mV and the area-specific resistance between 700 and 900 °C of these cells are listed in Table 4. From this table it is clear that the area-specific resistance decreased and thus the current density increased with increasing grain size of the cathode.

3.3. On the influence of CFL and CCCL thickness

3.3.1. Microstructural parameters

Cells with various thicknesses of the CFL and CCCL were produced. The CCCL was prepared by using paste CCCL-F with thickness variations between 10–20 and 70–75 μm. The CFL was based on paste CFL-A4 with a thickness varying between 10 and 40 μm (Table 5).

3.3.2. Microstructure

Micrographs of the fracture surface of single cells with various thicknesses of the CFL and the CCCL are shown in Fig. 4. From top to bottom the following layers can be observed: an LSM CCCL; an LSM/YSZ-type CFL, an YSZ electrolyte, a Ni/YSZ anode functional layer (AFL), and a Ni/YSZ substrate.

3.3.3. Current–voltage measurements

The first series of measurements deals with the influence of thickness variations of the CCCL on the current density and area-specific resistance. The thickness of the CFL was 10 μm. The current densities at 700 mV and the area-specific resistance are listed in Table 5. With increasing thickness of the CCCL (from 10–20 to 45–50 μm) an almost 20% decrease of the area-specific resistance was obtained. This decrease resulted in an increase of the current density. A further increase of the thickness did not have any further beneficial effect on the area specific resistance.

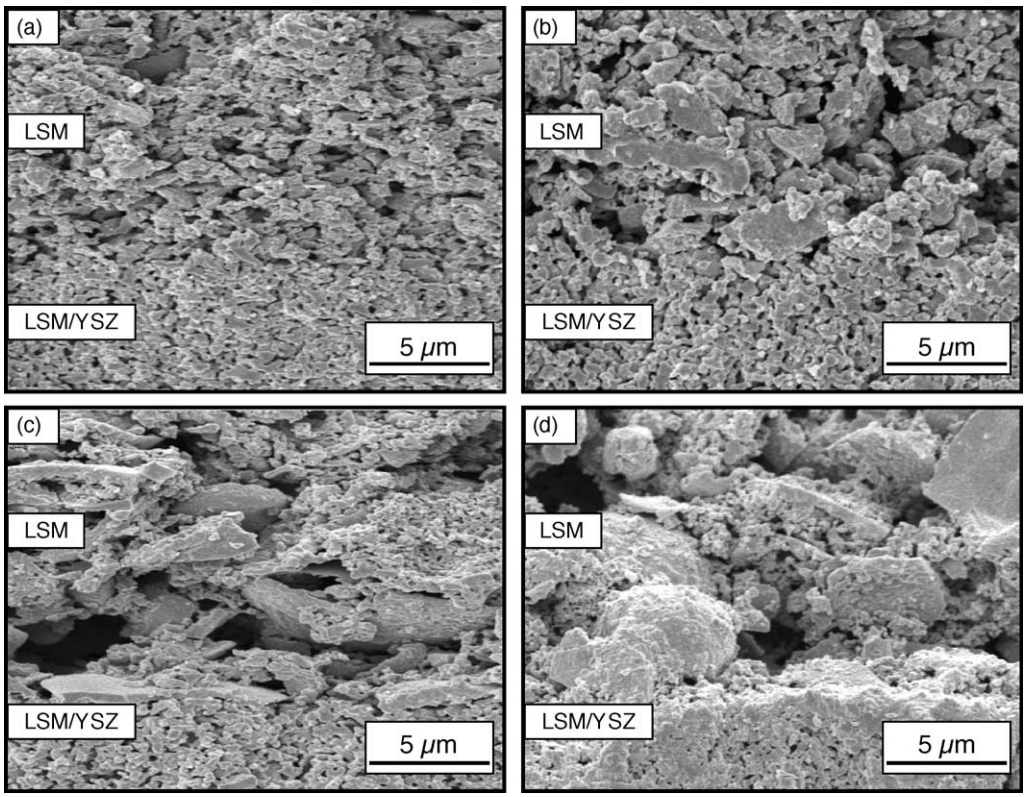

Fig. 3. SEM micrographs of the fracture surface of single cells with the same CFL (CFL-A6) and different CCCLs. The CCCL was prepared by using the following pastes: (a) CCCL-C; (b) CCCL-B; (c) CCCL-E; (d) CCCL-F.

The other series of single cells was produced to optimise the thickness of the CFL. The thickness of the CCCL was 10–20 μm. An increase of the thickness of the CFL from 10 to 40 μm resulted in an increase of the area-specific resistance. As a result, a slightly lower current density was calculated.

The highest electrochemical performance was obtained with single cells with a thickness of the CFL and CCCL of 10 and 50–60 μm, respectively. With this combination a current density of $1.46 \pm 0.01\ A\ cm^{-2}$ was measured at 800 °C and 700 mV. By way of illustration, the current density at 800 °C and 700 mV as a function of the thickness of the two layers is shown in Fig. 5.

3.4. On the influence of YSZ calcination

3.4.1. Microstructural parameters

One series of cells was prepared pastes CFL-B2 (non-calcined YSZ) and CCCL-C, and CFL-A6 (calcined YSZ) and CCCL-C.

Table 4
Average calculated current densities and area-specific resistance between 700 and 900 °C of anode-supported single cells with a CFL (CFL-A6) and a CCCL as a function of the grain size of the CCCL paste

Temperature (°C)	2.47	3.09	4.69	10.2	26.0
Current density ($A\ cm^{-2}$ at 700 mV) as a function of the d_{90} (μm) of the CCCL paste					
900	1.84 ± 0.03	1.82 ± 0.21	1.94 ± 0.07	2.00 ± 0.05	2.05 ± 0.10
850	1.52 ± 0.06	1.55 ± 0.14	1.64 ± 0.05	1.69 ± 0.03	1.71 ± 0.02
800	1.12 ± 0.07	1.13 ± 0.09	1.21 ± 0.02	1.26 ± 0.01	1.27 ± 0.01
750	0.71 ± 0.07	0.74 ± 0.05	0.76 ± 0.01	0.82 ± 0.01	0.83 ± 0.02
700	–	–	–	0.50 ± 0.01	0.50 ± 0.01
Area-specific resistance ($m\Omega\ cm^2$) as a function of the d_{90} (μm) of the CCCL paste					
900	166 ± 2	165 ± 2	156 ± 6	150 ± 2	144 ± 3
850	195 ± 2	190 ± 3	184 ± 2	178 ± 3	180 ± 4
800	263 ± 3	254 ± 3	237 ± 3	224 ± 3	221 ± 2
750	425 ± 10	390 ± 8	380 ± 8	318 ± 5	360 ± 7
700	–	–	–	551 ± 14	555 ± 18

Table 5
Average calculated current densities and area-specific resistance of single cells as a function of the thickness of the CFL (CFL-A4) and CCCL (CCCL-F)

Temperature (°C)	Current density (A cm^{-2} at 700 mV) as a function of the thickness of the CFL and CCCL			
	CFL to CCCL (10 to 10–20 μm)	CFL to CCCL (10 to 45–50 μm)	CFL to CCCL (10 to 50–60 μm)	CFL to CCCL (10 to 70–75 μm)
900	1.62 ± 0.04	2.17 ± 0.14	2.04 ± 0.01	2.17 ± 0.01
850	1.45 ± 0.02	1.82 ± 0.04	1.83 ± 0.01	1.85 ± 0.02
800	1.12 ± 0.01	1.35 ± 0.02	1.38 ± 0.01	1.40 ± 0.02
750	0.76 ± 0.01	0.87 ± 0.02	0.91 ± 0.01	0.91 ± 0.01
700	0.49 ± 0.01	0.50 ± 0.01	0.57 ± 0.01	0.54 ± 0.01
	Current density (A cm^{-2} at 700 mV) as a function of the thickness of the CFL and CCCL			
	CFL to CCCL (10 to 10–20 μm)	CFL to CCCL (30 to 10–20 μm)	CFL to CCCL (40 to 10–20 μm)	CFL to CCCL (30 to 50–60 μm)
900	1.62 ± 0.04	1.58 ± 0.04	1.31 ± 0.04	2.17 ± 0.06
850	1.45 ± 0.02	1.40 ± 0.06	1.14 ± 0.04	1.90 ± 0.04
800	1.12 ± 0.01	1.07 ± 0.04	0.87 ± 0.03	1.46 ± 0.01
750	0.76 ± 0.01	0.71 ± 0.02	0.57 ± 0.01	0.99 ± 0.01
700	0.49 ± 0.01	0.42 ± 0.02	0.35 ± 0.01	0.59 ± 0.01
	Area-specific resistance (mΩ cm^2) as a function of the thickness of the CFL and CCCL			
	CFL to CCCL (10 to 10–20 μm)	CFL to CCCL (10 to 45–50 μm)	CFL to CCCL (10 to 50–60 μm)	CFL to CCCL (10 to 70–75 μm)
900	186 ± 2	133 ± 1	140 ± 1	138 ± 2
850	210 ± 2	170 ± 3	164 ± 3	163 ± 1
800	266 ± 2	212 ± 3	199 ± 3	207 ± 2
750	428 ± 7	346 ± 7	260 ± 5	305 ± 5
700	630 ± 27	610 ± 18	486 ± 13	531 ± 9
	Area-specific resistance (mΩ cm^2) as a function of the thickness of the CFL and CCCL			
	CFL to CCCL (10 to 10–20 μm)	CFL to CCCL (30 to 10–20 μm)	CFL to CCCL (40 to 10–20 μm)	CFL to CCCL (30 to 50–60 μm)
900	186 ± 2	191 ± 2	229 ± 2	153 ± 2
850	210 ± 2	221 ± 2	267 ± 1	166 ± 2
800	266 ± 2	287 ± 3	368 ± 6	214 ± 2
750	428 ± 7	454 ± 7	615 ± 8	327 ± 5
700	630 ± 27	821 ± 17	1024 ± 23	496 ± 18

In addition, a second series of cells were produced with a CCCL type F, which implies a significantly larger grain size. The CFL was again based on CFL-A6 and CFL-B2. The physical and chemical parameters (viscosity, grain size, grain size distribution, etc.) of CFL-A6 and CFL-B2 were similar. The thickness of the CFL and CCCL was 10 and 30–35 μm, respectively.

A third series was based on calcined (CFL-A4) or non-calcined (CFL-B1). Here, two different thicknesses, i.e. 10 and 30 μm, were applied. The thickness of the CCCL was 50–60 μm (CCCL-F).

3.4.2. Microstructure

Microstructural investigations showed that the microstructure of the CFL was not affected by using non-calcined YSZ instead of calcined YSZ. In both cases the microstructure appeared like in Fig. 3a.

3.4.3. Current–voltage measurements

The average current densities at 700 mV and the area-specific resistance of cells with a CFL prepared with calcined and non-calcined YSZ are given in Tables 6 and 7. These cells differ from each other by the two different types of CCCL, i.e. CCCL-C and CCCL-F.

The data listed in Table 6 show that the use of non-calcined instead of calcined YSZ did not affect the current density and area-specific resistance of the two series. Furthermore, from Table 7 it can be concluded that using single cells with an LSM/YSZ mass ratio of 50/50, the influence of the physical condition of the YSZ powder (calcined or non-calcined) to be used for the CFL was more pronounced. Here, for cells with a CFL and CCCL thickness of 10 and 50–60 μm, respectively, the use of non-calcined YSZ resulted in a slight decrease of the electrochemical performance. Instead, using cells with a CFL and CCCL thickness of 30 and 50–60 μm, respectively, a slight increase of the performance was obtained.

4. Discussion

The initial parameter for optimisation of the CFL was the variation of the LSM/YSZ mass ratio. The thickness of this

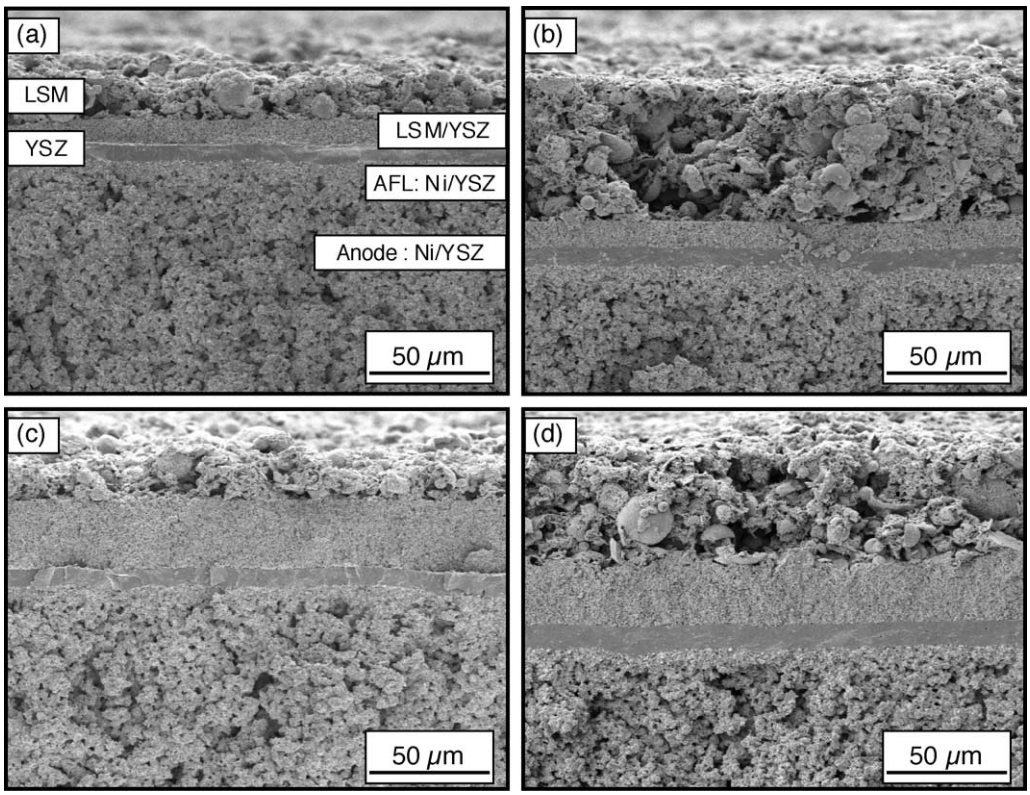

Fig. 4. SEM micrographs of the fracture surface of single cells with different thicknesses of the CFL (CFL-A4) and CCCL (CCCL-F). CFL:CCCL thickness: (a) 10 μm:10–20 μm; (b) 10 μm:50–60 μm; (c) 30 μm:10–20 μm; (d) 30 μm:50–60 μm.

layer was kept constant at 10 μm. This thickness was chosen since Wilkenhöner et al. [49] reported a strong increase of the overpotentials for the CFL (LSM/YSZ mass ratio: 60/40) with a thickness of less than about 10 μm. In that case involving a layer thickness between 10 and 35 μm, no obvious changes were found in the electrochemical activity. This was explained by the fact that a further increase of the total effective length of the triple phase boundary does not contribute to a higher performance. Similar features were found by Kenjo and Nishiya [2], who reported that the reciprocal polarisation resistance of an LSM/YSZ mass ratio of 33/67 composite electrode layer increased asymptotically with thickness up to about 10–15 μm. Juhl et al. [7] found that up to about 11 μm the polarisation resistance decreases with increasing thickness of the composite layer. This was explained by a limited percolation of ions and electrons when the thickness was less than 10 μm. Therefore, it can be expected that in the case of a thickness of the CFL of at least 10 μm, small differences in thickness do not significantly affect the electrochemical performance. This also means that differences in the electrochemical performance of cells with varied LSM/YSZ mass ratios are only attributed to differences in the composition

Table 6
Average calculated current densities and area-specific resistance of single cells with calcined and non-calcined YSZ (in CFL)

Temperature (°C)	CFL-B2–CCCL-C (YSZ not calcined)	CFL-A6–CCCL-C (YSZ calcined)	CFL-B2–CCCL-F (YSZ not calcined)	CFL-A6–CCCL-F (YSZ calcined)
Current density (A cm^{-2} at 700 mV) for calcined and non-calcined YSZ (CFL)				
900	1.77 ± 0.01	1.84 ± 0.03	2.03 ± 0.05	2.05 ± 0.10
850	1.49 ± 0.01	1.52 ± 0.06	1.72 ± 0.03	1.71 ± 0.02
800	1.08 ± 0.01	1.12 ± 0.07	1.29 ± 0.02	1.27 ± 0.01
750	0.71 ± 0.01	0.71 ± 0.07	0.83 ± 0.01	0.83 ± 0.02
700	–	–	0.50 ± 0.02	0.50 ± 0.01
Area-specific resistance (mΩ cm^2) for calcined and non-calcined YSZ (CFL)				
900	172 ± 1	166 ± 2	148 ± 1	144 ± 3
850	206 ± 4	195 ± 2	174 ± 1	180 ± 4
800	272 ± 5	263 ± 3	215 ± 5	221 ± 2
750	421 ± 8	425 ± 10	333 ± 7	360 ± 7
700	–	–	537 ± 15	555 ± 18

Thickness of CFL and CCCL was 10 and 30–35 μm, respectively.

Table 7
Average calculated current densities and area-specific of anode-supported single cells in relation to calcined and non-calcined YSZ (CFL)

Temperature (°C)	CFL-B1 to CCCL-F (10 to 50–60 μm (YSZ not calcined))	CFL-A4 to CCCL-F (10 to 50–60 μm (YSZ calcined))	CFL-B1 to CCCL-F (30 to 50–60 μm (YSZ not calcined))	CFL-A4 to CCCL-F (30 to 50–60 μm (YSZ calcined))
Current density (A cm^{-2} at 700 mV) for calcined and non-calcined YSZ (CFL)				
900	1.81 ± 0.04	2.17 ± 0.06	2.20 ± 0.02	2.04 ± 0.01
850	1.60 ± 0.01	1.90 ± 0.04	1.91 ± 0.05	1.83 ± 0.01
800	1.23 ± 0.01	1.46 ± 0.01	1.50 ± 0.05	1.38 ± 0.01
750	0.81 ± 0.01	0.99 ± 0.01	1.03 ± 0.04	0.91 ± 0.01
700	0.52 ± 0.04	0.59 ± 0.01	0.63 ± 0.06	0.57 ± 0.01
Area specific resistance (mΩ cm^2) for calcined and non-calcined YSZ (CFL)				
900	162 ± 2	140 ± 1	134 ± 1	153 ± 2
850	187 ± 2	164 ± 3	160 ± 2	166 ± 2
800	227 ± 3	199 ± 3	188 ± 2	214 ± 2
750	363 ± 6	260 ± 5	267 ± 4	327 ± 5
700	555 ± 15	486 ± 13	484 ± 11	496 ± 18

Thickness of CFL was 10 and 30 μm. Thickness of CCCL was 50–60 μm.

whereas the effect of small deviations in the thickness of the cathode functional layer can be excluded.

As regards the series of cells with a mass ratio of YSZ/LSM ranging between 30/70 and 70/30, the highest performance was obtained with a mass ratio of 50/50. These results corresponds well with those from Kenjo and Nishiya [2], who reported that the polarisation resistance of the LSM–YSZ composite cathode depends on the YSZ/LSM mass ratio, with the lowest corresponding to a mass ratio of 50/50. This was explained by the fact that a maximum of the total effective area, in this case the effective length of the triple-phase boundary, reached when both compounds are mixed in equal amounts. However, this is only true for similar grain sizes of both components. Other microstructures might have different optimal ratios. For example, Ostergard et al. [6] reported that in the case of composite electrodes made with a mixture of fine and coarse grains, the lowest polarisation resistance was obtained with a mass ratio of YSZ/LSM of 40/60. Tsai and Barnett [4] investigated two different types of

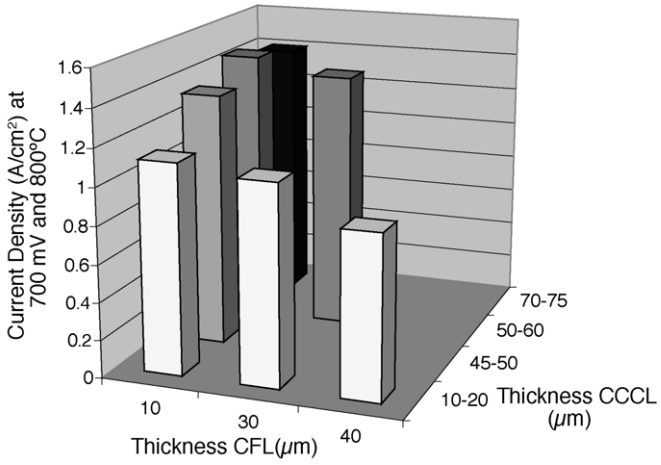

Fig. 5. Current density of LSM-based single cells at 800 °C and 700 mV as a function of thickness of the CFL (CFL-A4) and CCCL (CCCL-F).

LSM, i.e. $La_{0.8}Sr_{0.2}MnO_3$ and $(La_{0.8}Sr_{0.2})_{0.9}MnO_3$, which were mixed with YSZ. In the case of $La_{0.8}Sr_{0.2}MnO_3$, the lowest interfacial resistance was obtained with a mass ratio of YSZ/LSM of 60/40, whereas with $(La_{0.8}Sr_{0.2})_{0.9}MnO_3$ the optimum was obtained with a mass ratio 50/50.

Another series of measurements was based on systematically varying the mean grain size of the LSM CCCL. Results have shown that the current density was increased by increasing the mean grain size of the cathode. A similar relation between grain size and electrochemical properties was also found by Ostergard et al. [6] by studying the influence of structure and composition of LSM on the performance of fuel cells. Those experiments were based on a $La_{0.85}Sr_{0.15}Mn_yO_{3-\delta}$ cathode with a YSZ electrolyte. The electrode resistance was measured by impedance spectroscopy at 1000 °C and $pO_2 = 0.21$ atm. It was found that the polarisation resistance for coarse-grained LSM was lower than that for fine-grained LSM. This improvement of the polarisation resistance was correlated with a higher porosity allowing oxygen diffusion through the LSM layer to the triple-phase boundaries located in the inner LSM–YSZ layer. Tsai and Barnett [4] studied the effect of cathode composition, processing and microstructure on the performance of anode-supported cells with an LSM cathode and YSZ electrolyte. Here, it was found that cells with a porosity of 22 and 40% showed initially (at low current densities) similar behaviour, but after passing a critical current density, the cell voltage of the cell with the lower porosity dropped rapidly, which was ascribed to mass transport limitations of the oxidant.

Results from the present study show that the electrochemical performance improves with increasing grain size of the CCCL. However, conductivity measurements of the CCCL performed at 800 °C, revealed that the highest conductivity (90 S cm^{-1}) was related to the CCCL with the smallest grain size, whereas the lowest (35 S cm^{-1}) corresponded with a CCCL with the largest grain size. This means that the effect of an increased pore size of the CCCL on the electrochemical performance, facilitating the oxygen diffusion through

the CCCL layer to the inner CFL, dominates the decrease of the electronic conductivity.

It is expected that also the thickness of the CCCL can significantly influence the overall electrochemical performance of solid oxide fuel cells. In the case that the thickness of the current collector is too small in relation to the distance between the contact points of the Pt-mesh, it cannot be ensured that the current is collected from the whole LSM/LSM–YSZ interface area. This means that at least a minimum thickness of the LSM layer is needed to fully utilize the total surface area of the interface. Table 5 shows that the area-specific resistance was reduced (by almost 20%) by increasing the thickness of the CCCL from 10–20 to 45–50 μm. This might indicate that with a thickness of 10–20 μm, the total electrode area was not yet fully utilized. Based on these results it is recommended to apply a CCCL with a thickness of at least 45–50 μm in order to maximise the electrochemical performance.

In addition, thickness variations of the CFL can also significantly influence the electrochemical performance of solid oxide fuel cells. It has already been discussed that above a critical thickness of the CFL the electrochemical performance was more or less maximised [2,7,49] and did not further improve with increasing thickness. Instead, it can be expected that a CFL with a much larger thickness also might adversely influence the electrochemical performance due to longer diffusion paths for gas. Indeed, the experimental results showed that the performance with increasing thickness of the CFL was slightly decreased.

From these conclusions it is recommended to prepare single cells using a CFL with a thickness of at least 10 μm.

The aim of using non-calcined YSZ was to simplify the production route. On the one hand, reduction of the total number of steps in the processing procedure results in a decrease of production costs. On the other hand, using non-calcined YSZ for the CFL might induce a higher overall sintering activity affecting the electrochemical performance beneficially or detrimentally. A consideration of cells based on a CFL with an LSM/YSZ mass ratio of 60/40 revealed no obvious differences, neither between the microstructure of the CFL prepared with calcined or non-calcined YSZ, nor in the electrochemical performance.

In the case of single cells with an LSM/YSZ mass ratio of 50/50, the influence of the use of non-calcined YSZ was more obvious. However, the electrochemical performance was still satisfactory, indicating that non-calcined YSZ can be a potential candidate to be used for the CFL. In other words, the production route of LSM single cells can be simplified by using non-calcined YSZ without a significant detrimental effect on the electrochemical performance.

5. Conclusions

- Results from electrochemical measurements presented here showed that the performance of LSM-based solid oxide fuel cells can be improved by varying the LSM/YSZ mass ratio of the CFL. Using LSM and YSZ powders with similar grain sizes, the optimum LSM/YSZ mass ratio was determined at 50/50, thus maximising the effective length of the triple phase boundary where the cathode material, the electrolyte material and gas are in contact with each other.
- A further increase of the electrochemical performance was obtained by increasing grain size of the CCCL. The highest performance was achieved with non-ground LSM powder, which, adventitiously, also simplifies the production route.
- Results showed that also the thickness of the CFL and CCCL affects the current density. With respect to the CFL, at least a thickness of 10 μm is needed to maximise its utilisation. In case of the CCCL, a thickness of at least 45–50 μm is needed.
- The maximum current density at the tested temperatures and 700 mV was obtained on single cells with a CCCL having a thickness of 50–60 μm, and $d_{90,LSM}$ = 26.0 μm, a CFL with an LSM/YSZ (non-calcined) mass ratio of 50/50, a thickness of 30 μm, and $d_{90,LSM}$ = 0.9 μm.

Acknowledgements

The present study was financially supported by the German Federal Ministry of Economics and Labour (BMWA) under contract no. O327088C/8-1A. The authors thank Mr. W. Jungen for the synthesis of the spray-dried LSM, Mr. M. Kampel, and Mr. G. Blaß for the preparation of anode substrates and electrolytes, Mrs. B. Röwekamp and Mr. H. Wesemeyer for performing the electrochemical measurements.

References

[1] H.P. Buchkremer, U. Dieckmann, D. Stöver, Proceedings of the Second European Solid Oxide Fuel Cell Forum, Oslo, Ulf Bossel, May, 1996, p. 221.
[2] T. Kenjo, M. Nishiya, Solid State Ionics 57 (1992) 295–302.
[3] E.P. Murray, T. Tsai, S.A. Barnett, Solid State Ionics 110 (1998) 235–243.
[4] T. Tsai, S.A. Barnett, Solid State Ionics 93 (1997) 207–217.
[5] M.J. Jorgensen, S. Primdahl, M. Mogensen, Electrochemica Acta 44 (1999) 4195–4201.
[6] M.J.L. Ostergard, C. Clausen, C. Bagger, M. Mogensen, Electrochemica Acta 40 (1995) 1971–1981.
[7] M. Juhl, S. Primdahl, C. Manon, M. Mogensen, J. Power Sources 61 (1996) 173–181.
[8] N.T. Hart, N.P. Brandon, M.J. Day, N. Lapena-Rey, J. Power Sources 106 (2002) 42–50.
[9] (a) N.T. Hart, N.P. Brandon, M.J. Day, J.E. Shemilt, J. Mater. Sci. 36 (2001) 1077–1085;
(b) J. Akikusa, K. Adachi, K. Hoshino, T. Ishihara, Y. Takita, J. Electrochem. Soc. 148 (11) (2001) A1275–A1278.
[10] Y.K. Lee, J.Y. Kim, Y.K. Lee, I. Kim, H.S. Moon, J.W. Park, C.P. Jacobson, S.J. Visco, J. Power Sources 115 (2003) 219–228.
[11] J. Akikusa, K. Adachi, K. Hoshino, T. Ishihara, Y. Tacita, J. Electrochem. Soc. 148 (11) (2001) A1275–A1278.

[12] K. Choy, W. Bai, S. Charojrochkul, B.C.H. Steele, J. Power Sources 71 (1998) 361.
[13] T. Fukui, S. Ohara, K. Murata, H. Yoshida, K. Miura, T. Inagaki, J. Power Sources 106 (2002) 142–145.
[14] K. Huang, J. Wan, J.B. Goodenough, J. Mater. Sci. 36 (2001) 1093–1098.
[15] J.P.P. Huijsmans, F.P.F. van Berkel, G.M. Christie, J. Power Sources 71 (1998) 107–110.
[16] J.W. Yan, Y.G. Lu, Y. Jiang, Y.L. Dong, C.Y. Yu, W.Z. Li, J. Electrochem. Soc. 149 (9) (2002) A1132–A1135.
[17] J.W. Erning, T. Hauber, U. Stimming, K. Wipperman, J. Power Sources 61 (1996) 205–211.
[18] L.G.J. de Haart, K. Mayer, U. Stimming, I.C. Vinke, J. Power Sources 71 (1998) 302–305.
[19] D. Kek, P. Panjan, E. Wanzenberg, J. Jamnik, J. Eur. Ceram. Soc. 21 (2001) 1861–1865.
[20] S. de Souza, S.J. Visco, L.C. De Jonge, Solid State Ionics 98 (1997) 57–61.
[21] V.V. Kharton, F.M. Figueiredo, L. Navarro, E.N. Naumovich, A.V. Kovalevsky, A.A. Yaremchenko, A.P. Viskup, A. Carneiro, F.M.B. Marques, J.R. Frade, J. Mater. Sci. 36 (2001) 1105–1117.
[22] E. Maguire, B. Gharbage, F.M.B. Marques, J.A. Labrincha, Solid State Ionics 127 (2000) 329–335.
[23] C. Lu, W.L. Worrell, R.J. Gorte, J.M. Vohs, J. Electrochem. Soc. 150 (3) (2003) A354–A358.
[24] M. Sahibzada, B.C.H. Steele, K. Zheng, R.A. Rudkin, I.S. Metcalfe, Catal. Today 38 (1997) 459–466.
[25] M. Sahibzada, B.C.H. Steele, K. Zheng, R.A. Rudkin, J.M. Bae, N. Kiratzis, D. Waller, I.S. Metcalfe, in: B. Thorstensen (Ed.), Proceedings of the Second European Solid Oxide Fuel Cell Forum, Oslo, Ulf Bossel, May, 1996, pp. 687–696.
[26] S. Wang, T. Kato, S. Nagata, T. Kaneko, N. Iwashita, T. Honda, M. Dokiya, Solid State Ionics 152/153 (2002) 477–484.
[27] C. Xia, F. Chen, M. Liu, Electrochem. Solid State Lett. 4 (5) (2001) A52–A54.
[28] B. Zhu, J. Power Sources 5071 (2002) 1–9.
[29] M. Sahibzada, S.J. Benson, R.A. Rudkin, J.A. Kilner, Solid State Ionics 113–115 (1998) 285–290.
[30] S.P. Simner, J.F. Bonnett, N.L. Canfield, K.D. Meinhardt, J.P. Shelton, V.L. Sprenkle, J.W. Stevenson, J. Power Sources 113 (2003) 1–10.
[31] S. Wang, T. Kato, S. Nagata, T. Honda, T. Kaneko, N. Iwashita, M. Dokiya, Solid State Ionics 146 (2002) 203–210.
[32] K. Sasaki, J. Tamura, M. Dokiya, Solid State Ionics 144 (2001) 233–240.
[33] S.P. Simner, J.F. Bonnett, N.L. Canfield, K.D. Meinhardt, J.L. Shelton, V.I. Sprenkle, J.W. Stevenson, Proceedings of the 2002 Fuel Cell Seminar FUEL CELL, Fuel Cells-Reliable, Clean Energy for the World, Palm Springs, CA, November 18–21, 2002, p. 344.
[34] M. Watanabe, H. Uchida, M. Shibata, N. Mochizuki, K. Amikura, J. Electrochem. Soc. 141 (1994) 342.
[35] H. Uchida, M. Yoshida, M. Watanabe, J. Electrochem. Soc. 146 (1999) 1.
[36] H. Uchida, S. Arisaka, M. Watanabe, Solid State Ionics 135 (2000) 347.
[37] K. Sasaki, J. Tamura, H. Hosoda, T.N. Lan, K. Yasumoto, M. Dokiya, Solid State Ionics 148 (2002) 551–555.
[38] K. Sasaki, J. Tamura, M. Dokiya, Solid State Ionics 144 (2001) 223–232.
[39] N. Khramushin, G. Mezheritsky, Y. Moskalev, I. Prilezhaeva, N. Soloviev, in: J. Huijsmans (Ed.), Proceedings of the Fifth European Solid Oxide Fuel Cell Forum, Lucerne, Switzerland, July 1–5, 2002, p. 385.
[40] T. Ishihara, S. Fukui, H. Nishiguchi, Y. Tacita, J. Electrochem. Soc. 149 (7) (2002) A823–A828.
[41] E.P. Murray, M.J. Sever, S.A. Barnett, Solid State Ionics 148 (2002) 27–34.
[42] A. Petric, P. Huang, F. Tietz, Solid State Ionics 135 (2000) 719–725.
[43] I. Taniguchi, R.C. van Landschoot, J. Schoonman, Solid State Ionics 156 (2003) 1–13.
[44] H. Tu, Y. Takeda, N. Imanishi, O. Yamamoto, Solid State Ionics 117 (1999) 277–281.
[45] K. Yasumoto, Y. Inagaki, M. Spiono, M. Dokiya, Solid State Ionics 148 (3–4) (2002) 545–549.
[46] C. Xia, W. Rauch, F. Chen, M. Liu, Solid State Ionics 149 (2002) 11–19.
[47] J.M. Ralph, A.C. Schoeler, M. Krumpelt, J. Mater. Sci. 36 (2001) 1161–1172.
[48] A.B. Stambouli, E. Traversa, Sustain. Energy. Rev. 6 (5) (2002) 433–455.
[49] R. Wilkenhöner, W. Malléner, H.P. Buchkremer, Th. Hauber, U. Stimming, in: B. Thorstensen (Ed.), Proceedings of the Second European Solid Oxide Fuel Cell Forum, Oslo, Norway, May 6–10, 1996, pp. 279–288.